The Grosmont: a complex dolomitized, fractured and karstified heavy oil reservoir in a Devonian carbonate-evaporite platform

Hans G. Machel*, University of Alberta, Edmonton, Alberta, T6G2E3
hans.Machel@ualberta.ca

Mary Luz Borrero, Husky Energy, Calgary, Canada
Eugene Dembicki, Athabasca Oil Sands Corp, Calgary, Canada
Harald Huebscher, Shell Canada, Calgary, Canada
Luo Ping, PetroChina, Beijing, China
and
Yi Zhao, Husky Energy, Calgary, Canada

GeoConvention 2012:Vision

Summary

The Upper Devonian Grosmont platform in Alberta, Canada, is the world's largest heavy oil reservoir hosted in carbonates, with 400-500 billion barrels of IOIP at an average depth of about 250 – 400 m. Our study, which aims to aid in thermal recovery of this reservoir, shows that the current reservoir characteristics were created by the succession of five major factors and/or processes: sedimentary stratigraphy, dolomitization, polyphase and polygenetic fracturing, polyphase and polygenetic karstification, and biodegradation. Most of the present porosity and permeability is due to fracturing and karstification.

The sedimentary stratigraphy of the Grosmont reservoir consists of 6 stacked carbonate units interbedded with marls and some evaporites. The latter two originally acted as aquitards during diagenesis but are breached or missing in parts of the area today. Dolomitization by density-driven reflux was the first pervasive diagenetic process. Most dolostones are fine-crystalline and tight, however, and the only notable porosity caused by and/or related to dolomitization is scattered molds and vugs. A dense fracture network was created in three or four phases. Most fractures probably originated from collapse following subsurface salt dissolution and/or from Laramide tectonics far to the west, whereby pulsed crustal loading in the fold-and-thrust belt created a dynamic forebulge in the Grosmont region via multiple pulses of basin-wide crustal flexing, each followed by relaxation. The fracture network probably was reactivated and/or expanded by glacial loading and post-glacial isostatic rebound in the Pleistocene and Holocene, respectively.

The region experienced three or four prolonged periods of epigene (top-down) karstification, although there is tangible evidence for only two of them in the Grosmont platform. The first of these episodes was a 'warm epigene karstification' during the Jurassic - Cretaceous, and the second was/is a 'cold epigene karstification' that started sometime in the Cenozoic and is continuing to this day, as is biodegradation. In addition, there is circumstantial evidence for hypogene (bottom-up) 'karstification' (= dissolution) throughout much of the geologic history of the Grosmont since the Late Devonian, with two possible maxima around the time of hydrocarbon emplacement, i.e., Early-Middle Cretaceous and Early Tertiary, respectively.

Introduction

Beneath the Cretaceous oil sands deposits of Alberta, Upper Devonian carbonates of the Nisku, Upper Ireton and the Grosmont Formations form a carbonate platform that hosts at least 400 billion barrels IOIP in the form of low-gravity (API ~5° to ~9°) bitumen (Hein and Marsh 2008; Wo et al 2011), by some estimates up to ~500 billion barrels. This renders the Grosmont the world's largest unconventional oil reservoir hosted in carbonates (Alvarez et al. 2006, 2008). The reservoir is located within the often cited 'carbonate triangle' that contains heavy oil reserves in carbonates at four stratigraphic levels: the Devonian Grosmont and Nisku, and the Mississippian Shunda and Debolt (AEUB 2007).

Geologically and physiographically the Grosmont reservoir is variably referred to as a platform or shelf or complex. It is approximately 150 km wide and at least 600 km in length and thus is almost as large as the Great Bahama Bank (Fig. 1). Seismic data define a relatively sharp depositional edge along its western and southern limits, whereas the eastern limit is erosional, and the northern limits are almost unknown. The region studied by our group encompasses Townships 60 to 90 and Ranges 19W4 to 12W5 (Fig. 1). Several strike and dip sections cover all stratigraphic levels and facies types, and they allow references to the underlying reefs that constitute the northernmost part of the Rimbey-Meadowbrook reef trend.

Stratigraphy and Deposition

The sedimentary stratigraphy of the Grosmont reservoir consists of six stacked carbonate units interbedded with marls and some evaporites (Fig. 2). Each of these stratigraphic units has shallowing-upward facies characteristics (Fig. 3), commonly with biostromal, open marine facies (tabular stromatoporoid floatstone to rudstone) at the base, followed by marginal marine, lagoonal and shoal deposits (*Amphipora* floatstone to rudstone; peloid, intraclast and/or bioclast packstone to grainstone), and then peritidal carbonate facies (laminated, algal-laminated and massive (dolo)mudstone) (Cutler, 1983; Machel and Hunter, 1994). Brecciated and reworked dolomudstone facies, indicative of short-lived supratidal conditions in parts of the carbonate platform, and/or interbedded carbonate mudstones and anhydrites cap some of the cycles. Thin, regionally extensive marl layers, commonly referred to as 'shale breaks', mark relatively short-lived flooding events at the beginning of each cycle. In some parts of the study area there is evidence of higher (fourth) order cyclicity in form of additional thin marly layers, which has prompted some workers to further subdivide the above stratigraphic units (for example the UGM3 into UGM 3a and UGM3b).

Layers of anhydrite and/or solution-collapse breccias suggestive of their former presence occur at the stratigraphic levels of the UGM1 and UGM3/Upper Ireton. These evaporites are referred to as the Hondo Formation or Member. Evaporitic deposition originally as gypsum is indicated by laminar, bedded, enterolithic and otherwise contorted anhydrite layers with thicknesses of a few cm to dm (Figs. 3F, 4A, 4B). There also are isolated occurrences of halite hopper molds (Fig. 3H). These textures suggest that evaporation on the platform commonly reached gypsum saturation and only occasionally halite saturation. Secondary/replacive anhydrite nodules and patches are also present (Fig. 4C) and most probably are diagenetically redistributed from the original depositional gypsum layers.

According to the Geologic Atlas of the Western Canada Sedimentary Basin (Mossop and Shetsen 1994), the Hondo occurs over a large region in the south-central part of the Grosmont platform (oval labeled HONDO in Fig. 1). However, evaporites should not form far out on a platform nearer to its edge than to the paleo-shoreline. Detailed wireline log correlation, logging of cores and drill cuttings revealed the reasons for this 'abnormal' evaporite distribution (Borrero and Machel 2009; Borrero 2010): the platform margin migrated from east to west through time. The first time Hondo evaporites were deposited was during deposition of the UGM1. At that time the Grosmont platform margin was located on top of the underlying Cooking Lake platform margin, and the Leduc reef(s) at the Cooking Lake margin formed a slight paleotopographic high that permitted evaporite deposition in the region to its east (Figs. 5, 6). The second time of recognizable evaporite deposition was during UGM3/Upper Ireton times, when the Grosmont platform margin was located much farther west. Latest by this time the Grosmont was no longer a platform proper but a ramp that graded into the basinal marls to the west, as shown by well log characteristics. But then subvertical, syndepositional faulting provided for a slightly raised margin, which enabled evaporation in a lagoon or salina on the platform (Figs. 5, 6).

Burial history

Comprehensive sedimentologic data from western Canada presented in Mossop and Shetsen (1994) suggests that the Grosmont region underwent two relatively rapid periods of subsidence, one from the Late Devonian to the Mississippian, the other from the middle Cretaceous to the Paleocene, with a long period of uplift, erosion, and subaerial exposure in between (Fig. 7). Estimated maximum burial depths are about 1700m in the western downdip part and about 800 m in the eastern updip part of the platform, which is now exposed and/or eroded. However, these burial depths are very poorly constrained from sedimentological data (thicknesses, erosional surfaces) farther west and south. It is quite possible if not likely that the actual maximum burial depths were much less than cited above during the Late Paleozoic (hence the dashed burial 'curves' and question mark between them in Fig. 7). In addition, following Blakey's (2011) paleogeographic maps for North America, most of Alberta may have been subaerially exposed from the Mississippian to the middle Jurassic. If true, this circumstance is of significance in the context of karstification (see below).

Throughout its history of repeated subsidence, uplift, and erosion, the Grosmont platform was affected by many diagenetic processes that partially overlapped in time and space (Fig. 8). The processes that most affected the current reservoir characteristics on a regional scale are/were dolomitization with partial subsequent recrystallization, fracturing, karstification, and biodegradation. Locally other processes were important, such as calcite or anhydrite cementation from redistribution of calcium sulfate, or sulfide reduction forming pyrite and elemental sulfur, which are present in a few cores.

Dolomitization

Hydrostratigraphic, petrologic, and geochemical data have been used to identify and delineate paleofluid flow and areas of cross-formational fluid flow in the Grosmont. The Cooking Lake platform/aquifer and the Leduc reefs sitting on top of this platform are completely dolomitized, as are the UGM2 and 3, whereas the LGM and UGM1 are only partially dolomitized and contain significant

amounts of limestone. Correlating with this apparent dichotomy, petrologic and geochemical data show that there were at least two dolomitization events caused by fluids of differing composition and hydrologic drives (Dolomite-1 and –2, Fig. 8).

Dolomite-1 in the UGM2 and 3 is stratiform, mostly fine-crystalline and fabric retentive (Fig. 3D-H). Most of these dolostones are tight except for scattered molds and vugs, and generally do not qualify as 'good' reservoir rocks. In contrast, dolomite-2 is medium to coarse-crystalline and occurs in the lower parts of the Grosmont and in the underlying Leduc and Cooking Lake Formations, in some locations cross-cutting the intervening LGM, which is otherwise undolomitized. These dolostones generally have significant intercrystal porosity, but most of the commercial bitumen saturation is located stratigraphically higher in the reservoir.

Taking the stratigraphic, petrologic and geochemical data together, it appears that dolomite-1 was formed by mesohaline reflux more or less syndepositionally during deposition of the UGM2 and UGM3. On the other hand, dolomite-2 probably was formed by ascending basinal brines (Huebscher 1996; Machel and Huebscher 2000; Jones et al. 2003; Huebscher and Machel 2004).

Fractures

Fractures are of great interest for any investigation of reservoir characteristics. In the Grosmont reservoir, the fractures will not only provide fluid pathways during thermal recovery, they probably will create increasing permeabilities during bitumen extraction (Wagner et al. 2010).

The Grosmont reservoir is pervasively fractured. For simplicity, this section describes the salient features of all types of fractures together. Petrographic and circumstantial evidence indicates that fractures were created in three or four phases (F1-F4: Figs. 7,8). Most fractures probably formed in the second and third phases (F2 and F3) and many were reactivated in the last phase (F4). Diagenetic cements are generally absent in all types of fractures, while many appear enlarged by dissolution and/or are filled with bitumen.

In-situ subvertical fractures can be recognized in almost all Grosmont cores (Fig. 9A,B). In addition, many core intervals appear irregularly fractured into crackle breccias (Figs. 9C,D) or rubble (Fig. 10A) and other types of breccias that fall into several sub-types: syndepositional (from syndepositional evaporite dissolution and/or reworking by waves, thus not part of this discussion of fracturing); solution-collapse from post-depositional removal of evaporites (Figs. 10B,C) or from dissolution of carbonate; infills of karst (Fig. 9A?, Fig. 11); and mylonitic breccias along fault planes.

Wagner et al. (2010, 2011) found that the fractures are fractal and classified them into three 'families' that range in vertical scale from sub-cm to more than 100m, whereby the large-scale features were referred to as *'low-throw faults and fracture corridors'*. They did not offer genetic interpretations for the fracture systems that they identified. However, circumstantial reasoning allows us to provide a genetic interpretation for fractures of phases F2, F3, and F4 (discussed further below).

Fractures F1 are best recognized within, although not restricted to, clasts deposited in relatively wide fissures or caves. These fractures are almost invariably somewhat widened by dissolution (Fig. 9A). The age and cause for this phase of fracturing is indeterminate. All that can be said is that these fractures formed prior to the first phase of karstification K1, which is also indeterminate (Figs. 7,8 - further discussed below). Thus, fracturing F1 could have happened as early as the Mississippian or as late as the middle to upper Jurassic (Fig. 8).

Karstification

The Grosmont reservoir is pervasively karstified. The karst is fractal, in that individual karst features range in scale from tens of meters to sub-micrometers. Furthermore, the karst is polyphase and polygenetic, in that dissolution affected the platform multiple times and was driven by more than one process (K1-K5: Figs. 7,8).

Karst features On the largest scale karst features can be properly recognized only in seismic. The most prominent karst features at this scale are circular to oval sinkholes, between 30 and 150 m in diameter. They are located right below the regional sub-Cretaceous unconformity. In plan view the sinkholes appear to be almost randomly distributed (Fig. 12) and thus unpredictable.

On the scale of individual wells, caves can be recognized by a combination of neutron density and caliper log characteristics (Dembicki 1994; Dembicki and Machel 1996). In core, karst can be identified as solution-collapse breccias and intraformational breccia infills (Figs. 9, 10). Some breccias have clasts that appear to be partially rounded and cannot be correlated from well to well. These core intervals may have been deposited in cave streams. Other breccias appear to be stratiform and can be correlated over several townships. These breccias probably originated from evaporite dissolution and collapse under some sedimentary overburden. In addition, a few paleocaves contain extraformational infills, most notably Cretaceous coal and rare, whitish microcrystalline mixtures of kaolinite and quartz as the dominant minerals, as identified by XRD (Fig. 11). The latter probably originated as playa sediments in relatively recent times, which were washed into the caves below during flooding events. Similar sediments are formed in the playas of southeastern Alberta today, where episodic flooding occurs seasonally from snow melt in the spring or during storms in the summer and fall. On the smallest scale of investigation, karstification is evident by pervasive inter- and intracrystal dolomite dissolution, as shown in thin sections and SEM images.

Dolomite powder A highly unusual albeit relatively common rock type in the Grosmont is dolomite powder cemented with bitumen. In core this material is black to dark brown, depending on the color of the bitumen (Fig. 10D). It is sticky and commonly malleable to degrees ranging between pottery clay and plastic explosives, which led to various fanciful names including ‘dolo fudge’ and ‘dolo gunk’. When the bitumen is dissolved, all that remains is a nearly white to grey dolomite powder (Figs. 10E). Some core intervals with dolomite powder can be correlated over relatively large distances and appear to be stratiform in at least a part of the Grosmont platform.

Speculations as to the origin of this dolomite powder range from syndepositional calcite or dolomite dissolution, via syndepositional or postdepositional evaporite dissolution, to cryogenic mechanical weathering during Pleistocene interglacial periods. The latter interpretation, seemingly the oddest and

thus least likely one, is well supported by data from powderized dolostones in Triassic dolostones of the Buda Hills, Hungary (Poros et al. 2010, 2011; Poros 2011). At present, we cannot definitively tell how the dolomite powder in the Grosmont formed. On the balance of all data, we favor dissolution of gypsum or anhydrite layers, which are known to contain countless 'floating' dolomite crystals in some evaporite deposits elsewhere (Fig. 10F). Upon dissolution of the sulfates, these crystals would form a residue of dolomite powder. A cryogenic origin appears unlikely in case of the Grosmont, considering that the dolomite powder is bitumen-saturated, and that there were no cold climatic periods in the Grosmont region preceding oil migration. On the other hand, if the powdered dolomite in the Grosmont is indeed of a cryogenic origin, it would have been created during the Pleistocene, which would require that bitumen invaded the dolomite powder intervals sometime in a Pleistocene interglacial or even in the Holocene. This is not impossible, considering that oil/bitumen can re-migrate at any time after its original migration and emplacement.

Phases and timing The earliest karstification phase of the Grosmont may have happened during the Middle-Late Mississippian when karstification affected the United States and at least the southern perimeter of western Canada nearly continent-wide (Fig. 7: K1). At present there is no tangible evidence that this karstification affected the Grosmont platform, however.

A second phase of karstification in the Grosmont region may have happened during the Permian-Triassic (Fig. 7: K2), when Mississippian limestones in Manitoba acquired small solution features and mottling on an unconformity that is overlain by Lower Jurassic red beds and anhydrite. The Grosmont shelf, or at least its eastern perimeter, probably was exposed during this time interval also. However, there is no tangible evidence in the Grosmont for karstification during this Permian - Triassic period of exposure and erosion either.

A third, prolonged and definitely pervasive karstification phase that affected east-central Alberta was during the Late Jurassic - Early Cretaceous (Fig. 7: K3). Proof of this timing of karstification in the Grosmont region is provided by incised valleys and the numerous sinkholes along the regional sub-Cretaceous unconformity, which is overlain by Lower Cretaceous clastics. We herewith refer to this karstification as the 'warm epigene karstification' because the climate in what is now Alberta was relatively warm during those times as a result of a relatively warm global climate, and because the Alberta region was located at relatively low latitudes (Blakey 2011).

Regardless of whether or when epigene karstification affected the Grosmont platform, it was subjected to at least some dissolution from ascending waters that did not have a local meteoric origin. This process is also known as 'hypogene karstification' (Klimchouk 2007) (Fig. 7: K4; Fig. 8). *(Note: It may be preferable to avoid referring to basin-derived dissolution as 'karst', but the term 'hypogene karstification' is included herein because of its widespread popularity in the current technical karst literature).* The first argument in favor of dissolution from ascending brines is the widely acknowledged regional updip flow of basinal brines, which probably started as early as the latest Devonian and created, or was involved in, the formation of burial dolomites in the Cooking Lake platform and overlying Leduc reefs in the Grosmont region (see above). Further circumstantial evidence is derived from the fact that the Cooking Lake aquifer was a major migration route also for oil and gas, including organic acids in the front and CO_2 in the wake of the oil front, as well as H_2S from thermochemical sulfate reduction deeper in the basin, all of which would make basinal brines corrosive to carbonates and evaporites. It is likely, therefore, that the polyphase and polygenetic epigene karst system already identified gives way to a 'hypogene karst' system in the downdip part of the platform. If present, the

latter likely has different characteristics, i.e., most notably a maze system of passages rather than a stream system overlain by sinkholes. 'Hypogene karstification' of the downdip parts of the platform could have happened almost throughout the history of the platform since deposition but probably was most intense right before and after hydrocarbon emplacement when organic acids (before) and thermogenic CO_2 and H_2S (after) were being transported into the Grosmont platform (Fig. 7).

A fourth period of prolonged and pervasive epigene karstification began during the Tertiary and is continuing to this day at least in the updip part of the platform (Fig. 7: K5), even where buried under a few meters to perhaps 200-300m of Cretaceous clastics and Pleistocene-Holocene sediments. This phase of karstification may have started as early as the Upper Paleocene, when the ocean finally receded from the region, or later in the Tertiary. In any case, the climate in Alberta was somewhat colder than during the Cretaceous, trending toward very much colder during the Pleistocene glaciations. For these reasons, we refer to this second period of prolonged and pervasive karstification as the 'cold epigene karstification'. The effects on the Grosmont correspond to what Ford (1989) termed 'glacial rejuvenation of karst' elsewhere in Canada.

Cold epigene karstification could have affected the underlying carbonates by four processes: (1) glacial rejuvenation of paleokarst; (2) subglacial creation of karst landforms; (3) dissolution under permafrost; and (4) postglacial meltwater penetration. Processes 1, 3 and 4 probably were the most important. Glacial meltwater has been identified in the Grosmont platform by hydrogeochemical (TDS, elemental, isotopic) data (Grasby and Chen 2005). The main effects of this cold epigene karstification would have been to overprint and enhance the older warm epigene karst features, inasmuch as the rock surfaces (along dissolution voids of all sizes up to that of caves, joints and fractures) were not already covered or saturated with bitumen. Thus, the bitumen-saturated part of the reservoir probably was not affected by much additional dissolution. However, there may have been significant additional dissolution in the water leg below the bitumen. Furthermore, if there was any cryogenic powderization of dolomite rock, it would have been part of this cold karstification period.

Implications There are multiple implications of karstification for the design and execution of thermal recovery schemes. For example, how many levels of enhanced dissolution are there? Are the connected? Are there subvertial dissolution pipes that crosscut the marl and evaporite aquitards, thus connecting the various reservoir intervals? Our early mapping of caves from caliper/neutron density logs and cores suggested that there may be two levels of enhanced dissolution crosscutting the stratigraphy (Fig. 13). More recent data (unpublished) suggest, however, that enhanced dissolution may be stratiform in at least part of the platform, in which case dissolution may have happened earlier relative to development of the regional structural dip, or dissolution simply followed bedding planes of enhanced susceptibility. Either way, enhanced stratiform dissolution must have happened in intervals with Hondo evaporites, based on their much higher solubility compared to the carbonates and on the fact that there are breccia intervals near the eastern subcrop at the stratigraphic level of the Hondo farther west. This led Machel and Huebscher (2000) to suggest that the largest caves should be located where present or former Hondo evaporites are crossed by one or both levels of non-stratiform enhanced karstification (Fig. 13).

Fracturing from salt solution

Fracturing from dissolution of the underlying Middle Devonian evaporites is herewith designated to be the second possible fracturing phase and almost certainly the first pervasive one in the Grosmont platform (Fig. 7: F2; Fig. 8). This phase was driven by meteoric water invasion during the Late Jurassic-Early Cretaceous that karstified the overlying Upper Devonian carbonates. Thus, dissolution of the Middle Devonian evaporites is part of karstification K3 *sensu strictu*. Fracturing K2 is singled out not for separation in timing but for separation in space and stratigraphic level.

It is generally acknowledged that salt solution affected the Middle Devonian evaporites that underlie the Upper Devonian Grosmont and the Cretaceous clastics in the Grosmont-Athabasca region (e.g. Page 1974; Mossop and Shetson 1994; Stanton 2004). Based on regional isopach mapping, the Middle Devonian evaporites wedge out eastward, starting a few townships west of the Athabasca River valley. The westernmost limit of salt solution can be regarded as the limit of a north-south trending 'hingeline zone' that was a few townships wide, above which the Upper Devonian section was subjected to stresses similar to those above normal faults in extensional tectonic regimes. This likely created swarms of fractures and faults similar to tectonic 'flower stuctures'. East of this hingeline zone, solution collapse probably created a more irregular stress field and fracture pattern in the overburden.

Tectonic Fracturing

Tectonic fracturing is herewith recognized as another major phase in the history of the Grosmont platform and designated as F3 (Figs. 7, 8). Interpretation of this phase rests on a comprehensive metastudy of the structural and sedimentologic history of the western United States and Canada by Miall et al. (2008) and studies cited therein.

The Laramide orogenesis began during the Late Campanian or Maastrichtian throughout much of the United States and climaxed during the Maastrichtian to Eocene, and foreland fold-thrust tectonism continued until the Early Paleogene. The importance of Laramide orogenesis for the Grosmont lies in the concomitant formation of a foreland bulge as a result of the large-scale flexure of the crust roughly parallel to the tectonic front. As the tectonic front moved generally eastward through time, so did the forebulge. The axis of the forebulge was located right under the Grosmont platform during the latest Cretaceous to Paleocene/Eocene (Catuneanu et al. 1999, 2000). Furthermore, episodes of flexural loading alternated with episodes of relaxation (Miall et al. 2008). This, then, probably was a principal cause for the creation of the fracture pattern(s) now observed in the Grosmont platform: pulses of uplift and relaxation of the forebulge during the Late Cretaceous to Paleocene/Eocene.

It is further noteworthy that a dense network of fractures and lineaments in the basement of the Alberta Basin is known from gravimetric and aeromagnetic studies (Lyatsky 2003; Lyatsky et al. 2005). The major two orientations WNW-ESE and NNE-SSW of these structural elements are recognizable also in the large-scale fracture system of the Grosmont. Thus, it appears that the Laramide-aged tectonic flexing of the foreland bulge reactivated at least some of the older structural elements in the basement.

Oil migration and emplacement

The most comprehensive treatment to date of this subject is by Higley et al. (2009) who evaluated the basin with a four-dimensional petroleum systems model in terms of the seven most likely source rocks, their maturation, timing of oil migration and emplacement, and the relative contributions of each source rock to the updip reservoirs. In the present context, the most important result of Higley et al.'s study is the time of hydrocarbon emplacement in the reservoir, which they determined to be between 90-40 m.y. ago, with the bulk of oil emplacement having taken place in the window of 70-50 m.y. ago (Fig. 7). Equally important, Higley et al. (2009) determined that most oil was derived from source rocks in the Jurassic Fernie Group (Gordondale Member and Poker Chip A shale) rather than from Devonian or Carboniferous sources, which were assessed to have contributed only very minor amounts of oil. Based on the radiometric studies by Selby and Creaser (2005) the Paleozoic source rock contribution may have arrived in the Grosmont region as early as 118-108 m.y. ago. Bennett et al.'s (2010) biomarker study affirmed that at least some of the Grosmont bitumen was sourced from the Carboniferous Exshaw Formation.

Glaciogenic Fracturing

Glaciogenic fracturing was the last of four fracturing events that affected the Grosmont platform (Fig. 7: F4; Fig. 8). The joints and fractures formed by the processes discussed earlier (F2-F3) must have been rejuvenated during glacial loading and post-glacial rebound in the Pleistocene/Holocene. The Pleistocene glaciations are known to have piled up enormous ice masses, which coalesced to the Laurentide ice sheet that covered all of Alberta for extended periods of time. The maximum thickness of glacial ice in the Grosmont region probably reached 1-2 km, while the thickness exceeded 4 km near the center of the Laurentide ice sheet in the Hudson Bay region (Paterson 1972; Marshall et al. 2000; Dyke et al 2000). The load of the ice first depressed the underlying strata, which then rebounded isostatically during and after the final ice melt, which occurred between about 15,000 and 6,000 years ago. The amounts of depression and isostatic rebound have been calculated to range between about 150 and 400m in the Hudson Bay region (Paterson 1972) and were proportionally less in the Grosmont region.

The question arises how significant glaciogenic stresses were for the Grosmont reservoir. A key observation in this regard is that almost none of the fractures in the reservoir are occluded by diagenetic minerals (also noted by Wagner et al 2010). This finding suggests that the glaciogenic stresses largely reactivated older joints and fractures and probably formed few new ones. However, the older fractures may have been widened significantly, causing enhanced permeability and bitumen re-migration. The overall significance of the glaciogenic movements for the reservoir remains speculative at this time.

Biodegradation and bitumen properties

Early organic geochemical studies found that the bitumens in the Cretaceous oil sands and in the Grosmont reservoir are similar in composition, suggesting a common origin, and that they are strongly to severely biodegraded (*e.g.*, Vigrass, 1968; Deroo *et al.*, 1977; Mackenzie *et al.*, 1983). More

recently, Bennett et al (2010) asserted that the biomarker characteristics of the Grosmont bitumen resemble those of the Carboniferous Exshaw source rock, implying that the Grosmont was sourced from the Exshaw, and they affirmed the severe degree of biodegradation in the Grosmont.

Our own biomarker work (Zhao 2009; Zhao and Machel 2011) indicates that the Grosmont reservoir was subjected to extreme levels of biodegradation, featured by the loss of regular steranes, strongly biodegraded hopanes, and affected distributions of tricyclics and diasteranes. The rare geological marker compound 28, 30-bisnorhopane is highly biodegraded but is prevailing in the Grosmont bitumen samples examined, supporting the notion that the Devonian carbonate bitumen and the Cretaceous oil sands have a common origin. The data show that the biodegradation is likely more intense around stratigraphic boundaries and generally increases from southeast to northwest (Fig. 14).

Several recognized biodegradation parameters, such as 17a(H)-hopane / 17a(H)-norhopane, are correlatable with the petrophysical properties of bitumen, especially viscosity (Zhao 2009; Zhao and Machel 2012). The viscosity distribution in the Grosmont reservoir is complex and varies cyclically with depth, commonly by one order of magnitude (Fig. 15). Moreover, viscosity seems related to stratigraphy, as similar trends are observed in samples from adjacent wells in the Nisku, Upper Ireton, and the Grosmont Formations, respectively. Lateral variations support the observations from vertical viscosity variations. Each stratigraphic unit appears to have its own viscosity distribution pattern.

Sweet Spots

In early 1994 two of us (Dembicki and Machel) endeavored to identify ‘sweet spots’ for thermal recovery, i.e., locations within the Grosmont reservoir that would be most profitable. To this end, a series of maps was produced for each stratigraphic level and overlain: structure, isopach of each reservoir unit, as well as hydrocarbon pore volume, isopach of the top seal/shale break, and proximity to overlying gas accumulations (some of which were being commercially exploited in the 1990s). The results of two of these sets of maps are shown in Figure 16, i.e., for the UGM2 and the Nisku. It is interesting to note that both ‘sweet spots’ are located within the area leased by Shell in 2006 for $465million. To this day Dembicki and Machel silently cry themselves to sleep some nights for not leasing those sweet spots themselves.

Acknowledgements

The various individual studies that contributed to this composite were supported by Agreement #800 from AOSTRA (Alberta Oil Sands Technology and Research Authority); consecutive Research and Discovery grants and a Strategic Grant from NSERC (Natural Sciences and Engineering Research Council of Canada) to HGM; a fellowship to HGM by the Alexander Humboldt Foundation; and by a number of oil companies, here listed in alphabetical order: AMOCO, CRESTAR, CHEVRON, ESSO, HOME OIL, HUSKY OIL, MOBIL, NORCEN, NUMAC, PAN CANADIAN, PETRO-CANADA, and SHELL, as well as by the Alberta Research Council.

References

AEUB 2007, Alberta's energy reserves 2006 and supply/demand outlook 2007-216. ST98-2007, 218 pp.

Alvarez, J.M., Escobar, E. and Ivory, J. 2006. Bibliographic Review of Carbonate Reservoirs. Heavy Oil & Oil Sands Internal Report, Alberta Research Council, March 2006.

Alvarez, J.M., Sawatzky, R.P. Forster, L.M., and Coates, R.M. 2008, Alberta's Bitumen Carbonate Reservoirs – Moving Forward with Advanced R&D. World Heavy Oil Congress, Edmonton 10-12 March 2008, Paper 2008-467, 14 pp.

Amthor, J.E., Mountjoy, E.W., and Machel, H.G., 1993, Subsurface dolomites in Upper Devonian Leduc Formation buildups, central part of Rimbey-Meadowbrook reef trend, Alberta, Canada. Bulletin of Canadian Petroleum Geology, v. 41, p. 164-185.

Bachu, S., 1999. Flow systems in the Alberta Basin: patterns, types and driving mechanisms. Bulletin of Canadian Petroleum Geology, v. 47, p. 455– 474.

Barret, K. and Hopkins, J. 2010, Stratiform Carbonate Breccias of the Grosmont Formation, Alberta. AAPG Search and Discovery Article #90108©2010 AAPG International Convention and Exhibition, September 12-15, 2010 Calgary, Alberta, Canada

Barrett, K., Hopins, J., Wilde, K.N. and Connelly, M.E., 2008, The Origin of Matrix and Fracture Mega-Porosity in a Carbonate Bitumen Reservoir, Grosmont Formation, Saleski, Alberta. World Heavy Oil Congress, Edmonton 10-12 March 2008, paper 2008-344, 11 pp.

Bennett B., Norka, I.M., Larter, S., and Ranger, M., 2010. The Application of oil-Source correlation tools towards understanding oil charge systematic in the carbonate reservoirs of northern Alberta. 2010 American Association of Petroleum Geologists International Conference and Exhibition Abstracts CD.

Blakey, R. 2011: http://www2.nau.edu/rcb7/globaltext2.html

Borrero, M.L., 2010, Hondo evaporites within the Grosmont heavy oil carbonate platform, Alberta, Canada. Unpub. M.Sc. Thesis, University of Alberta, 190 pp.

Borrero, M.L. and Machel, H.G. 2009, Hondo Evaporites in the Grosmont Heavy Oil Carbonate Reservoir. 2009 CSPG CSEG CWLS Convention, Calgary, Alberta, May 4-8 2009, p. 552-555.

Catuneanu, O., Sweet, A., and Miall, A. D., 1999, Concept and styles of reciprocal stratigraphies: Western Canada foreland system. Terra Nova, v. 11, pp. 1–8.

Catuneanu, O., Sweet, A., and Miall, A. D., 2000, Reciprocal stratigraphy of the Campanian–Paleocene Western Interior of North America. Sedimentary Geology, v. 134, pp. 235–255.

Dyke, A.S., Andrews, J.T., Clark, P.U., England, J.H., Miller, G.H. Shaw, J., and Veillette, J.J., 2002, The Laurentide and Innuitian ice sheets during the Last Glacial Maximum. Quaternary Science Reviews, v. 21, p. 9–31.

Cutler, W.G. 1983, Stratigraphy and sedimentology of the Upper Devonian Grosmont Formation, Alberta, Canada. Bulletin of Canadian Petroleum Geology, v. 31, p. 282-325.

Dembicki, E. A. 1994, The Upper Devonian Grosmont Formation: well log evaluation and regional mapping of a heavy oil carbonate reservoir in northeastern Alberta: M.Sc. thesis, University of Alberta, Edmonton, 221 p.

Dembicki, E.A. and Machel, H.G. 1996, Recognition and delineation of Paleokarst zones by the use of wireline logs in the bitumen-saturated Upper Devonian Grosmont Formation of northeastern Alberta, Canada. American Association of Petroleum Geologists Bulletin, v. 80, p. 695-712.

Deroo, G., Powell, T. G., Tissot, B., and McCrossan, R. G., 1977. The origin and migration of petroleum in the western Canadian sedimentary basin, Alberta; a geochemical and thermal maturation study. Geological Survey of Canada Bulletin, v. 262, p. 1-136.

Ford, D.C. 1989, Paleokarst of Canada. In: Bosak, P. (ed): Paleokarst - a systematic and regional review. Elsevier and Academia, Amsterdam and Praha, p.313-336.

Grasby, S.E. and Chen, Z. 2005, Subglacial recharge into the Western Canada Sedimentary Basin - Impact of Pleistocene glaciation on basin hydrodynamics. GSA Bulletin, v. 117 3/4, 500-514.

Hein, F.J. and Marsh, R.A. 2008, Regional geologic framework, depositional models and resource estimates of the oil sands of Alberta, Canada. World Heavy Oil Congress, Edmonton 10-12 March 2008, Paper 2008-320.

Higley, D.K., Lewan, M.D., Roberts, L.N.R. and Henry, M., 2009, Timing and petroleum sources for the Lower Cretaceous Manville Group oil sands of northern Alberta based on 4-D modeling. AAPG Bulletin, v. 93, p. 203-230.

Huebscher, H. 1996, Regional controls on the stratigraphic and diagenetic evolution of Woodbend Group carbonates, north-central Alberta. Unpub. Ph.D. Thesis, University of Alberta, 231 pp.

Huebscher, H. and Machel, H.G. 2004, Reflux and burial dolomitization in the Upper Devonian Woodbend Group of north-central Alberta, Canada. Dolomites - The Spectrum: Mechanisms, Models, Reservoir Development. CSPG Seminar and Core Conference, Jan 13-15 2004, Calgary, Alberta, Canada. Abstracts of Seminar Presentations, Core Displays and Posters: C017, 19 pages (CD-ROM). 12.

Jones, G.D., Smart, P.L., Whitaker, F.F., Rostron, B.J. and Machel, H.G. 2003, Numerical modeling of reflux dolomitization in the Grosmont platform complex (Upper Devonian), Western Canada sedimentary basin. American Association of Petroleum Geologists Bulletin, v. 87, p. 1273-1298.

Klimchouk, A., 2007, Hypogene speleogenesis: Hydrogeological and morphogenic perspective. National Cave and Karst Rsearch Inbstitute, Specail Paper No. 1, 106 pp.

Last, W.M, and Ginn, F.M. 2004, Saline systems of the Great Plains of western Canada: an overview of the limnogeology and paleolimnology. Open Access: *Saline Systems* 2005, 1:10 http://www.salinesystems.org/content/1/1/10, 38 pp.

Luo, P. and Machel, H.G. 1995, Pore size and pore-throat types in a heterogeneous Dolostone reservoir, Devonian Grosmont Formation, Western Canada Sedimentary Basin. American Association of Petroleum Geologists Bulletin, v. 79, p. 1698-1720.

Luo, P., Machel, H.G. and Shaw, J., 1994, Petrophysical properties of matrix blocks of a heterogeneous dolostone reservoir - the Upper Devonian Grosmont Formation, Alberta, Canada. Bulletin of Canadian Petroleum Geology, v. 42, p. 465-481.

Lyatsky, H.V. 2003, Catalogue of selected regional gravity and magnetic maps of northern Alberta. EUB/AGS Special Report 56, 43 pp.

Lyatsky, H.V. Pana, D.I., and Grobe, M. 2005, Basement structure in central and southern Alberta: Insights from gravity and magnetic maps. EUB/AGS Special Report 72, 83 pp.

Machel, H.G., and Hunter, I.G. 1994, Facies models for Middle to Late Devonian shallowmarine carbonates, with comparisons to modern reefs – a guide for facies analysis. Facies, v. 30. p. 155-176.

Machel, H.G., and Huebscher, H. 2000, The Devonian Grosmont heavy oil reservoir in Alberta, Canada. Zentralblatt für Geologie und Paläontologie, Teil I, Heft 1/2, p. 55-84.

Mackenzie, A. S., Wolff, G. A., and Maxwell, J. R., 1983. Fatty acids in some biodegraded petroleums; possible origins and significance; Advances in organic geochemistry, 1981. Proceedings of the International Meeting on Organic Geochemistry, p. 637-649.

Marshall, S.J., Tarasov, L., Clarke, G.K.C. and Peltier, W.R., 2000, Glaciological reconstruction of the Laurentide IceSheet: physical processes and modelling challenges. Canadian Journal of Earth Sciences, v. 37, p 769-793.

Miall, A.D., Catuneanu, O., Vakarelov, B.K., and Post, R., 2008, The Western Interior Basin. In: A.D. Miall (Ed.) The Sedimentary Basins of the United States and Canada. Sedimentary Basins of the World (Series Editor: K.J. Hsu), Elsevier, Amsterdam, p. 329-362.

Mossop, G.D., and I. Shetsen, I., compilers, 1994, Geologic Atlas of the Western Canada Sedimentary Basin. Canadian Society of Petroleum Geologists and Alberta Research Council.

Page, H.V., 1974, The environmental impacts of Alberta's tar sands industry, *in* L.V. Hills, ed., Oil Sands, Fuel of the Future: Canadian Society of Petroleum Geologists Memoir 3, p. 222-233.

Paterson, W. S. B. (1972), Laurentide Ice Sheet: Estimated volumes during Late Wisconsin, Reviews Geophysics, v. 10, p. 885–917, doi:10.1029/RG010i004p00885.

Poros, Z., 2011, Fluid migration and porosity evolution in the Buda Hills, Hungary – selected examples from Triassic and Paleogene carbonate rocks. Unpublished PhD Dissertation, Eötvös Lóránd University, Budapest, Hungary, 141 pp.

Poros, Z., Mindszenty, A., Machel, H.G., Ronchi, P. and Molnar, F., 2011, Powderization of Triassic dolostones in the Buda Hills, Hungary. Abstracts, 28th IAS Meeting of Sedimentology, 5-8 July 2011, Zaragoza, Spain, p. 535.

Poros, Z., Mindszenty, A., Machel, H.G., and Molnar, F., 2010, Powderization of Triassic dolostones in the Buda Hills, Hungary - an unusual type of karstification? Advances in Carbonate Exploration and Reservoir Analysis. The Geological Society, London, England, 4-5 November 2010, Book of Abstracts, p. 66-68.

Selby, D. and Creaser, R.A., 2005, Direct radiometric dating of hydrocarbon deposits using Rhenium-Osmium isotopes. Science, v. 308, p. 1293-1205.

Stanton, M.S. 2004, Origin of the Lower Cretaceous heavy oils ("tar sands") or Alberta. Search and Discovery Article # 10067 (on-line).

Switzer, S.B., Holland, W.G., Christie, D.S., Graf, G.C., Hedinger, A.S., McAuley, R.J., Wierzbicki, R.A., Packard, J.J., 1994, Devonian Woodbend-Winterburn strata of the Western Canada Sedimentary Basin. In: Geologic Atlas of the Western Canada Sedimentary Basin. G.D. Mossop and I. Shetsen (compilers). Calgary, Canadian Society of Petroleum Geologists and Alberta Research Council, p. 165-195.

Vigrass, l. W., 1968. Geology of Canadian heavy oil sands; Rocky Mountains-Breaking barrier boundaries. American Association of Petroleum Geologists Bulletin, v.52, p. 1984-1999.

Wagner, P.D., Nelson, R.A., Lonnee, J.S., Costello, M.S., Whale, R.H., McKinzie, W.J., Jennings, J.W., Balzarini, M.A., Reed, D.A., Al-Bhary, A.S., and Watson, R.C. 2010, Fracture Characterization of a Giant Unconventional Carbonate Reservoir, Alberta, Canada. AAPG Search and Discovery Article #90108©2010 AAPG International Convention and Exhibition, September 12-15, 2010 Calgary, Alberta, Canada.

Wagner, P.D., Nelson, R.A., Lonnee, J.S., Costello, M.S., Whale, R.H., McKinzie, W.J., Jennings, J.W., Balzarini, M.A., Reed, D.A., Al-Bahry, A.S., Watson, R.C, and Ortega, O. 2011. Natural fracture characterization of a giant unvonventional carbonate reservoir , Grosmont Venture, Alberta, Canada: implications for recovery. 14th Bathurst Meeting Abstracts. International Conference of Carbonate Sedimentologists, Bristol, England.

Wo, E., Song, L., Travis Hurst, T., and Sitek, N. 2011, Geological Review and Bitumen Resource Appraisal of the Grosmont Formation within the Athabasca Oil Sands Area. Search and Discovery Article #80130 (2011).

Zhao, Y., 2009, Petrophysical Properties of Bitumen from the Upper Devonian Grosmont Reservoir, Alberta, Canada. Unpub. M.Sc. Thesis, University of Alberta, 189 pp.

Zhao, Y. and Machel, H.G., 2011, Biodegradation characteristics of bitumen from the Upper Devonian Grosmont Reservoir, Alberta, Canada. Bulletin Canadian Petroleum Geology, 59 (2), p. 112-130.

Zhao, Y. and Machel, H.G., 2012, Viscosity and other rheological properties from the Upper Devonian Grosmont reservoir, Alberta, Canada. American Association of Petroleum Geologists Bulletin, 96(1), 133-153.

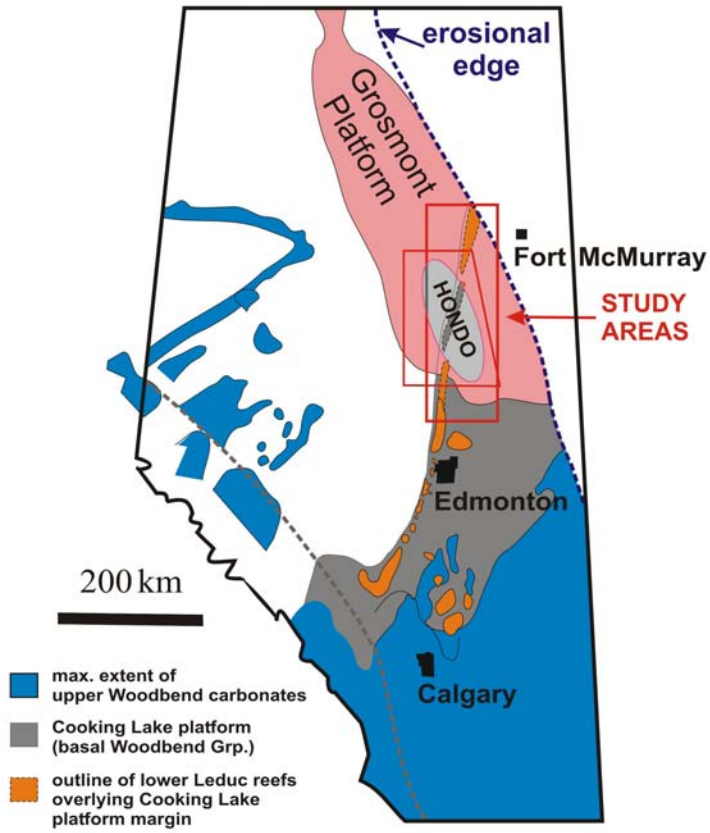

Fig. 1: Simplified subsurface map of the Upper Devonian Woodbend carbonate platforms and reefs in Alberta (modified from Switzer et al. 1994). Most of our studies were concentrated within the rectangle marked as study area. The Hondo study was conducted in the trapezoid study area.

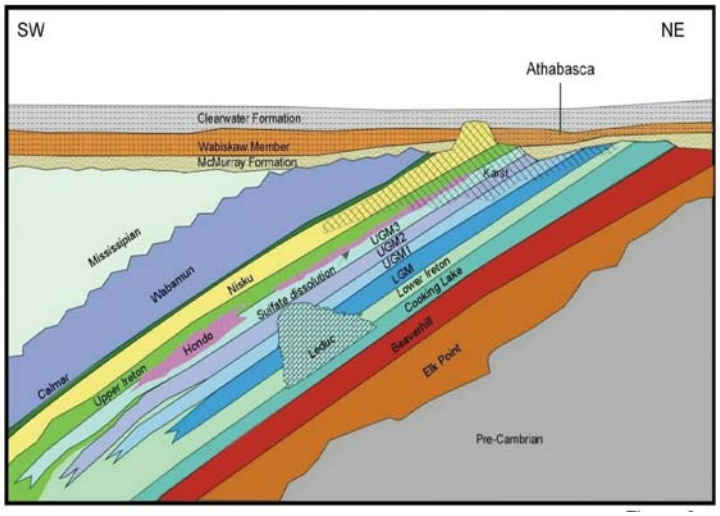

Fig. 2: Schematic SW-NW stratigraphic section across the study areas identified in Fig. 1.

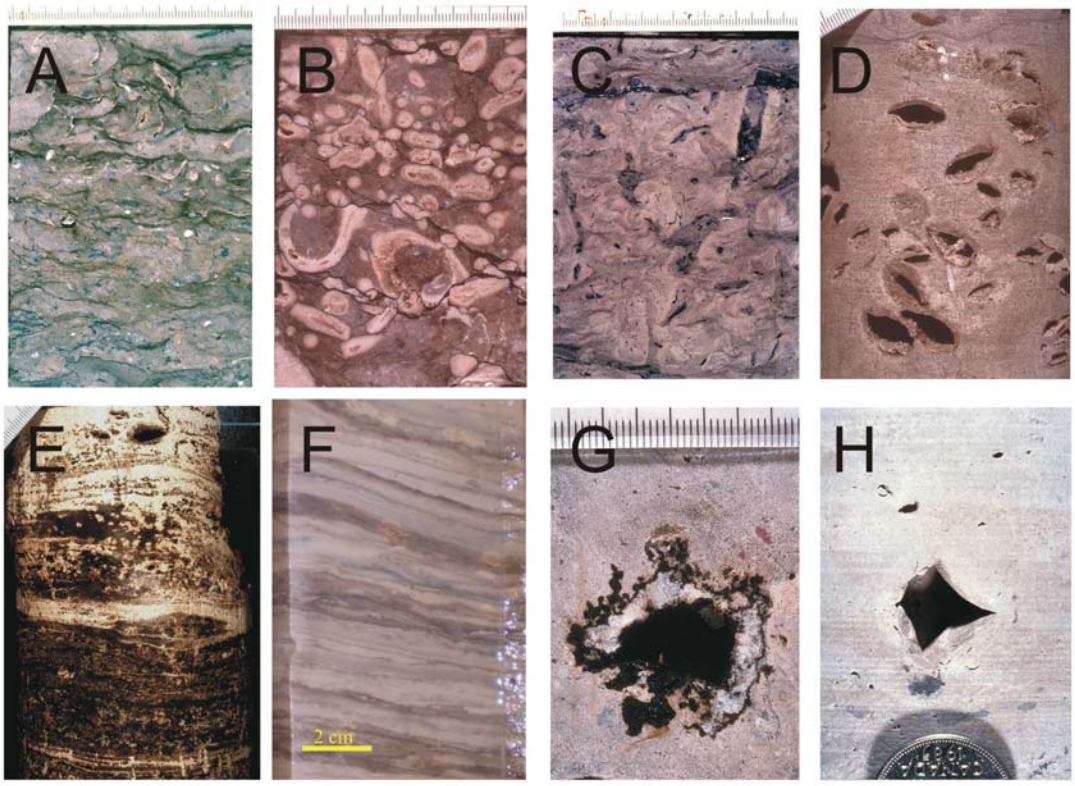

Fig. 3: Facies in an idealized shallowing-upward cycle of the Grosmont platform. A: subtidal skeletal grainstone facies; B,C,D shallower shelf facies; E: intertidal algal mat facies; F: brine pond anhydrite facies; G,H: supratidal muds with dissolved anhydrite nodule (G) and halite hopper mold (H).

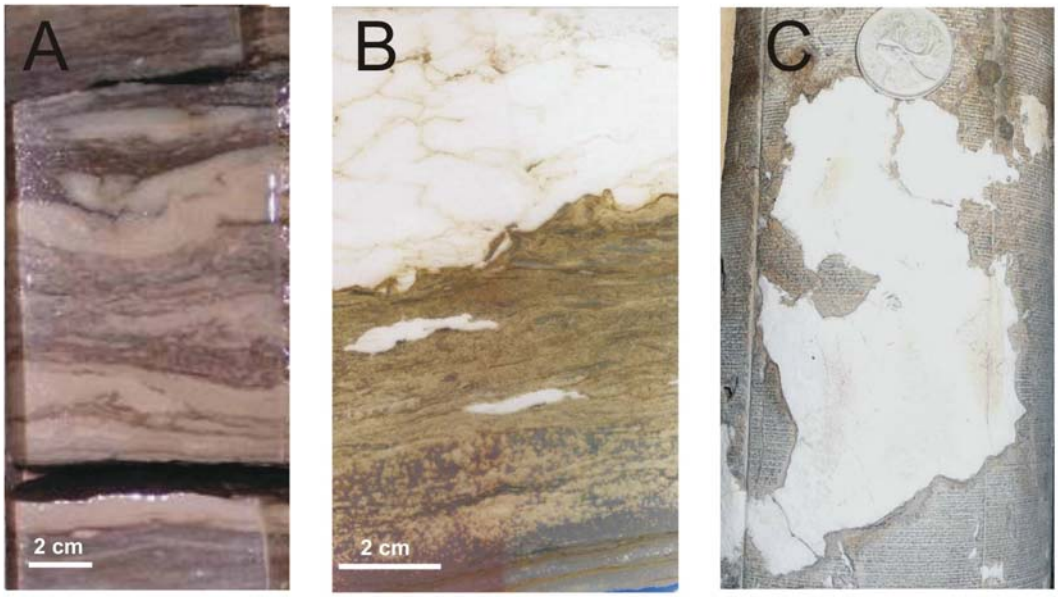

Fig. 4: A, B: 'Primary' subaqueous anhydrite facies; C: secondary/replacive anhydrite.

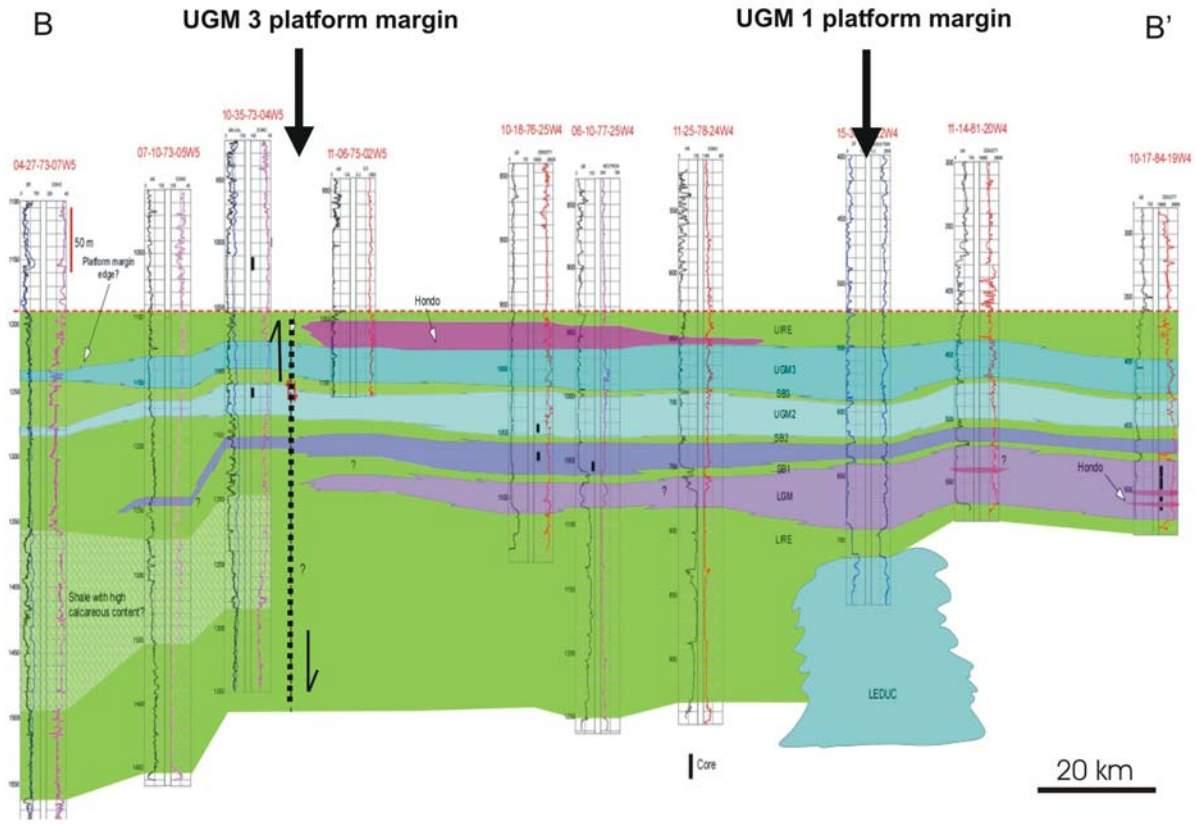

Fig. 5: Stratigraphic W-E section about midway through the Hondo area shown in Fig. 6. Note Hondo deposition at two stratigraphic levels: UGM1 and UGM3 and locations of corresponding platform/ramp margins. See text for further explanation.

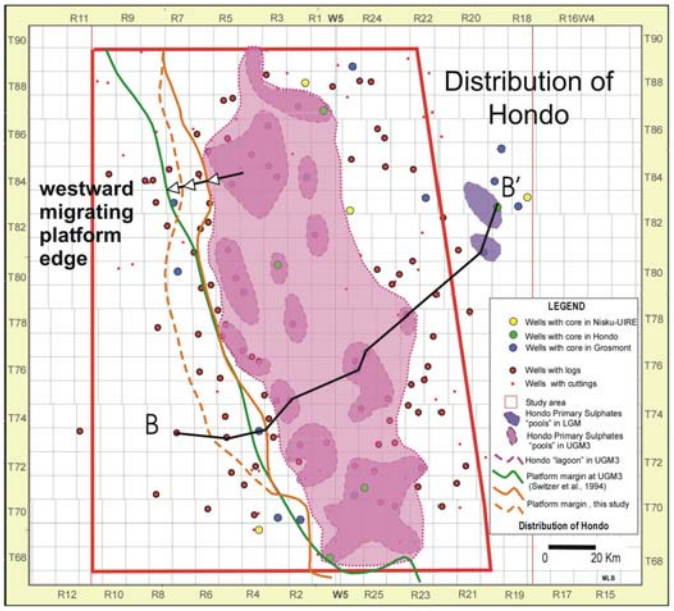

Fig. 6: Map of the Hondo area with well control and positions of platform margin/edge through time.

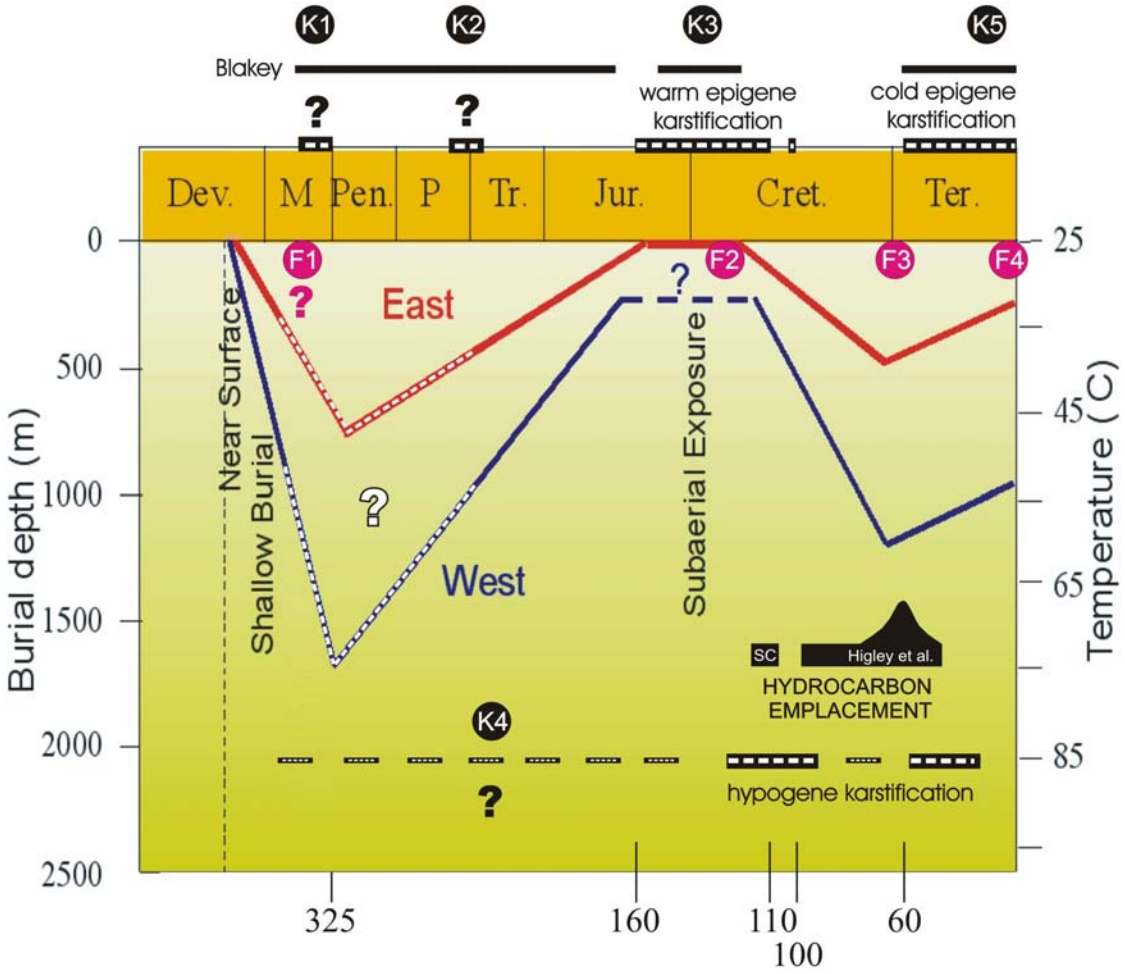

Fig. 7: Burial curve with interpreted periods of karstification (K1-K5) and fracturing (F1-F4). The red burial 'curve' is for the updip portion of the platform in the east, the blue 'curve' is for the downdip limit of the platform in the west. Black bars along the top labeled 'Blakey' designate periods of subaerial exposure according to Blakey's (2011) paleogeographic maps, while the black-and-white bars along the top mark periods of subaerial exposure of the updip portion of the Grosmont platform based on sedimentologic data in Mossop and Shetsen (1994) and Miall et al. (2008). Black-and-white bars along the bottom designate possible (narrow, ?) and likely (bold) periods of hypogene dissolution of the downdip part of the platform. Important times/periods as follows: from deposition to ~325 m.y. = relatively rapid burial to ~500 to max. 1,500 m in the downdip part of the platform (the amount of burial is poorly constrained and may have been much less); middle to late Mississippian: possible first epigene karstification; Late Permian to Early Jurassic: possible second epigene karstification; ~160 - 110 m.y.: warm epigene karstification; 110 - 103 m.y. minor marine transgression; 103-100 m.y. hiatus and possible subaerial exposure with karstification; 100 - 60 m.y.: mostly marine sedimentation, grading to fluvial in the last 8 - 5 m.y. of this time interval; ~60 m.y. to recent: subaerial exposure of the Grosmont region (Cretaceous clastics on top of the Devonian carbonates) with cold epigene karstification in the younger part of this time interval. Hydrocarbon emplacement probably began about 118-108 m.y. (Selby and Creaser 2005) or between 95-40 m.y., with peak emplacement by volume between 70-50 m.y. (Higley et al. 2009).

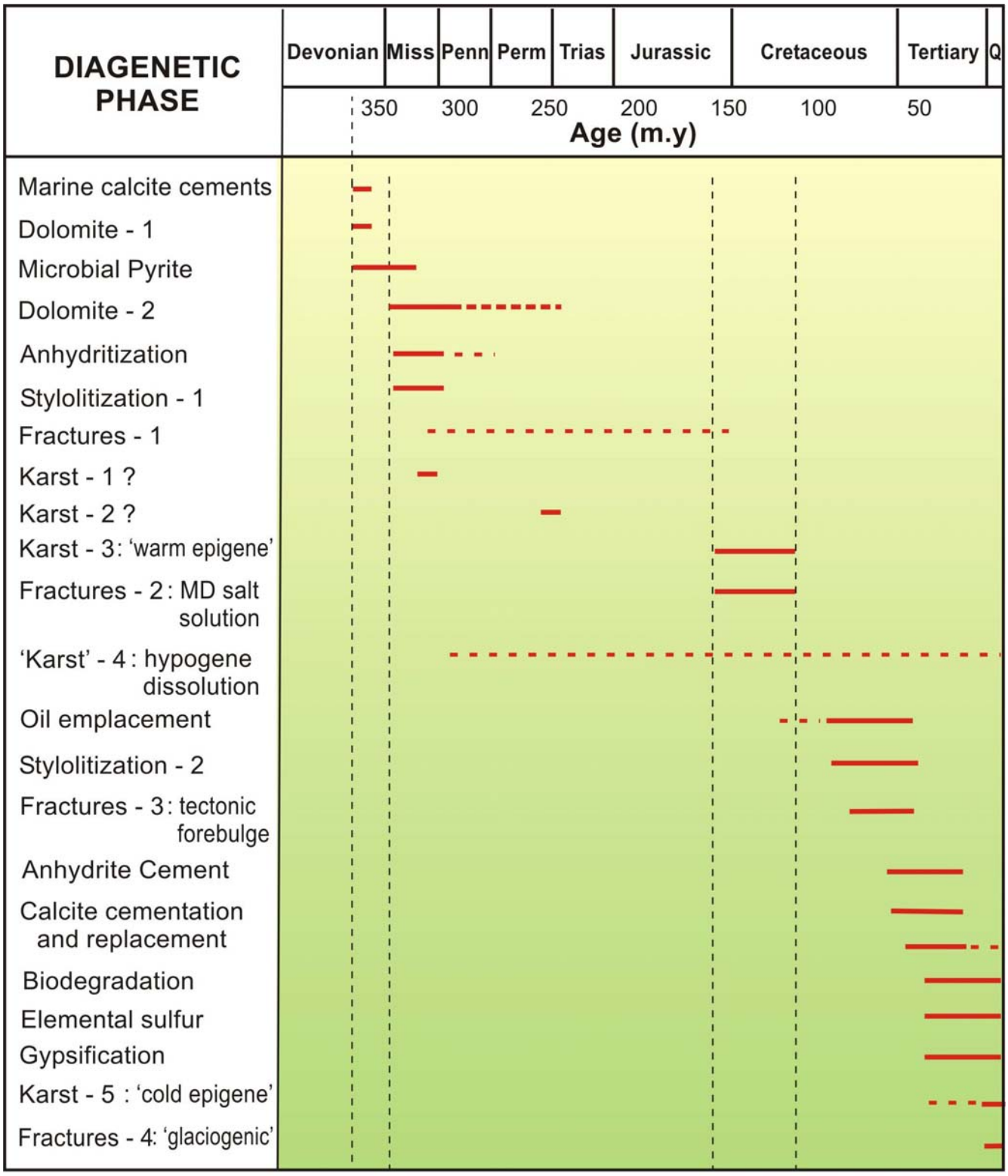

Fig. 8: Simplified paragenetic sequence for the Grosmont region. Correlate with Fig. 7.

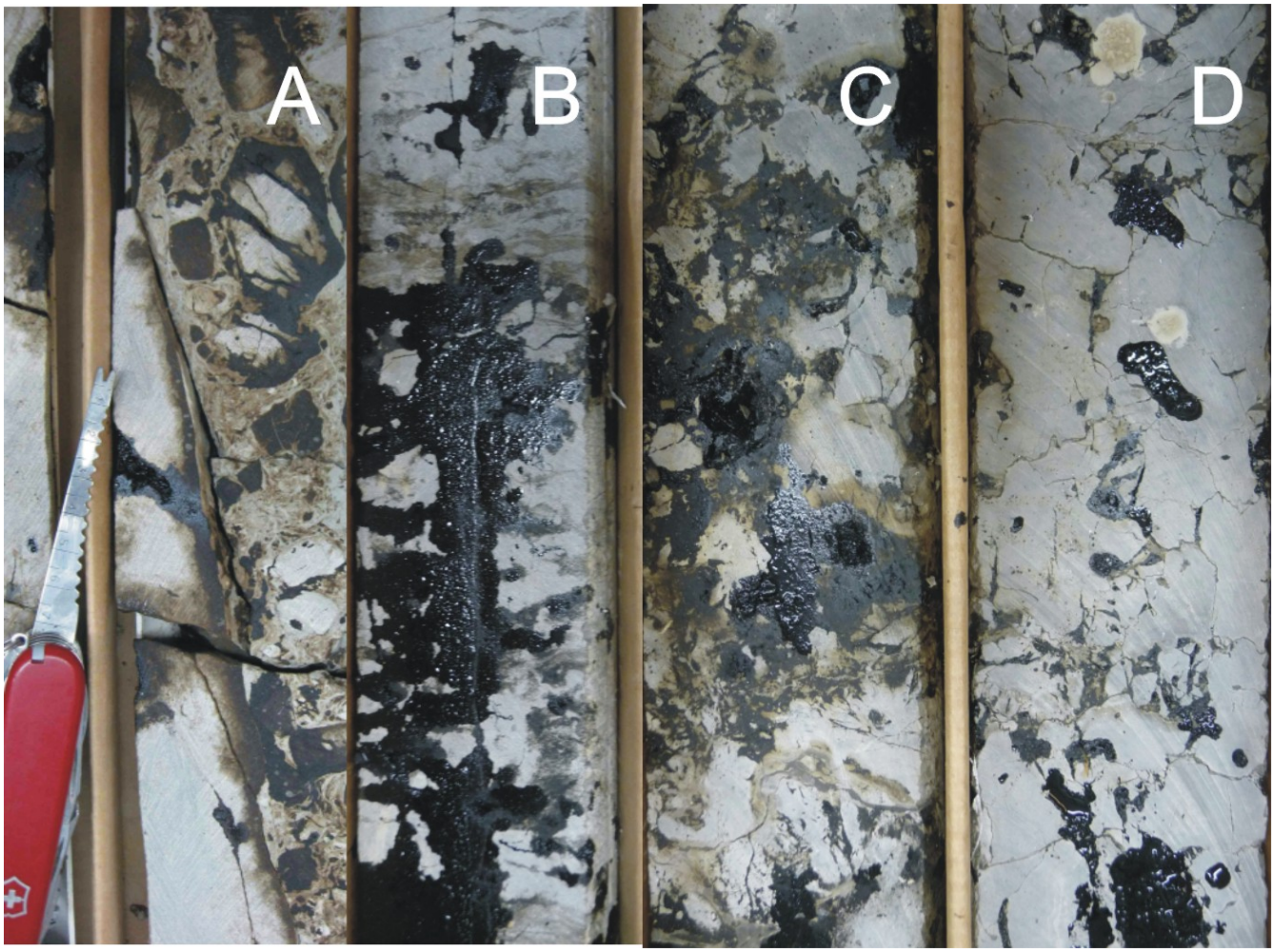

Fig. 9: A: Fracture/fault (or cave) with wall rock on left side and intraformational breccia (or cave infill) on the right. Note differential oil stain around and within clasts and in wall rock. Some clasts were fractured before being deposited in this breccia. Many clasts are bitumen-saturated while the matrix is not, suggesting oil migration and saturation before these clasts were deposited here. B: Bitumen oozing out of vertical hairline fracture, which is common in 'legacy cores' (drilled more than ~10 years ago) after a few years of storage. C,D: irreguar fracture network creating a 'crackle breccia' network.

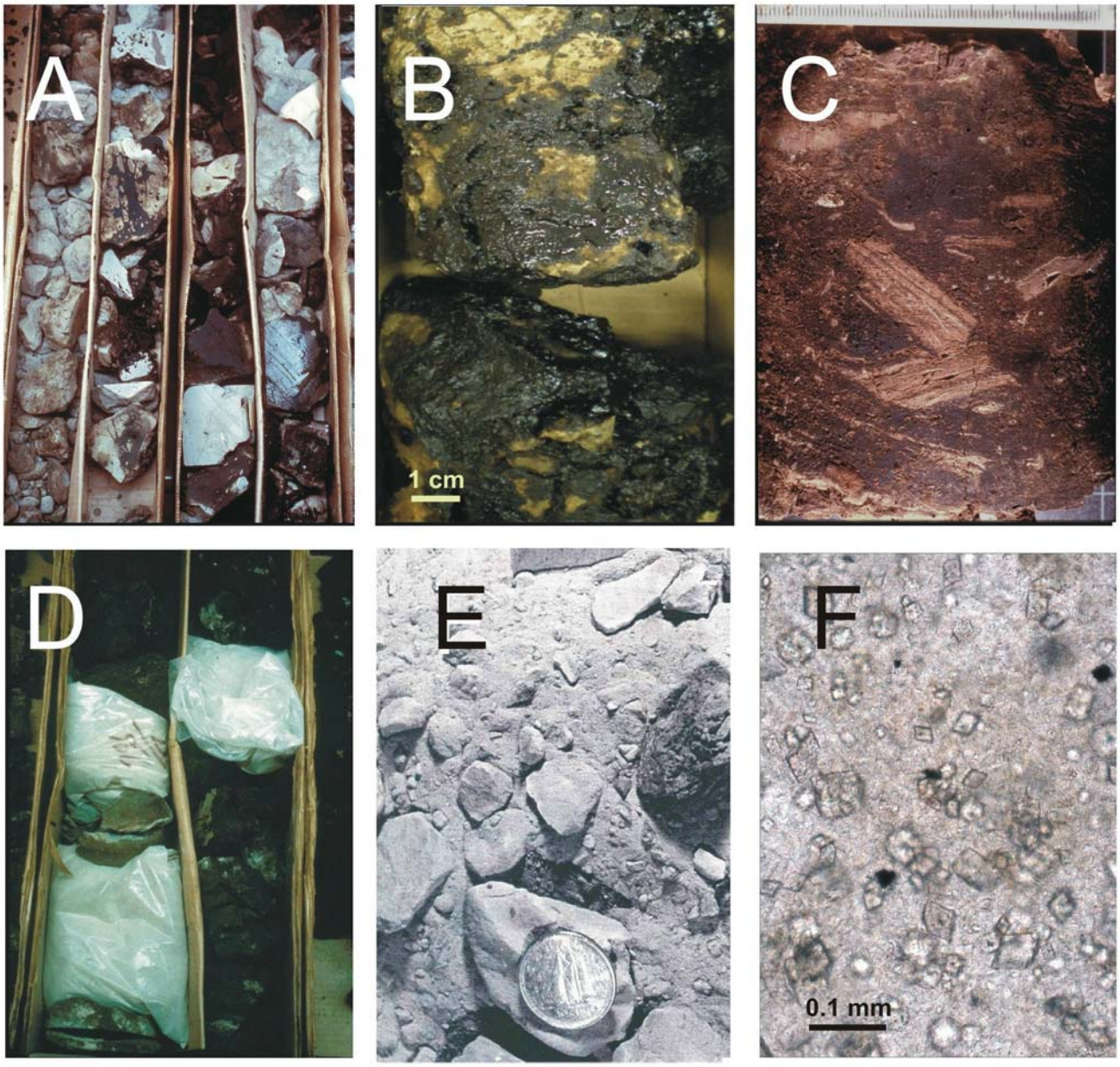

Fig. 10: A - C: Fractured and brecciated core intervals. D: Core interval with ‘dolo gunk’ = dolomite powder held together by bitumen. Bags contain white dolomite powder after bitumen extraction with organic solvent. E: Dolomite powder. F: Thin section, transmitted light: dolomite crystals floating in bedded anhydrite (Nisku Fm., township 14W4). This kind of rock is the most likely precursor of dolomite powder in the Grosmont.

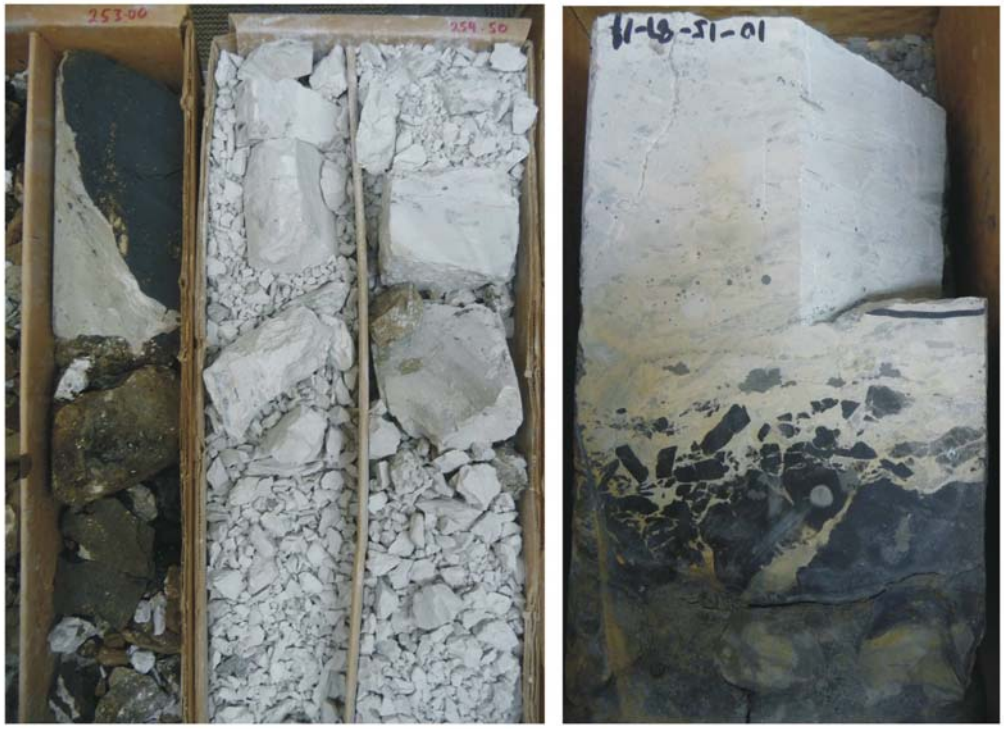

Fig. 11: Core interval with cave infill consisting almost entirely of microcystalline kaolinite and quartz, washed in from an overlying playa in relatively recent times.

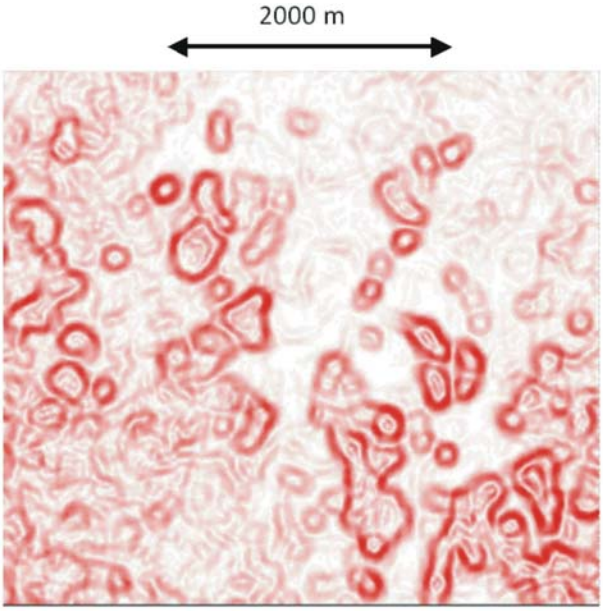

Fig. 12: Seismic image of sinkholes in a part of the Grosmont platform, showing their generally irregular distribution and variable sizes. Image obtained from Shell International and reproduced with permission.

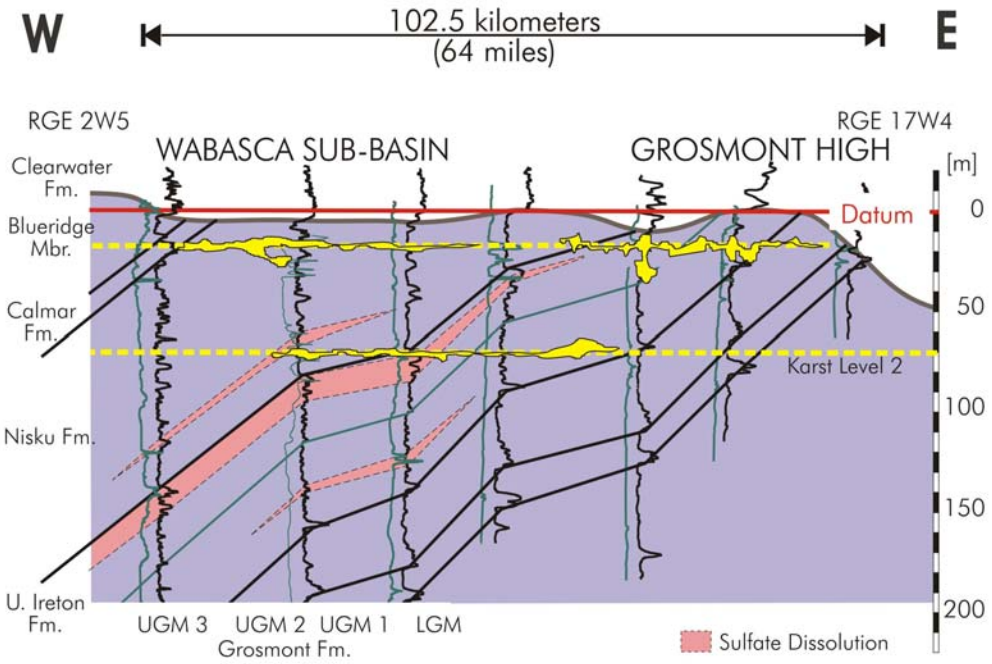

Fig. 13: Schematic W-E cross section though the central part of the study area, showing two levels of enhanced karst (cave?) formation and stratiform intervals of sulfate dissolution.

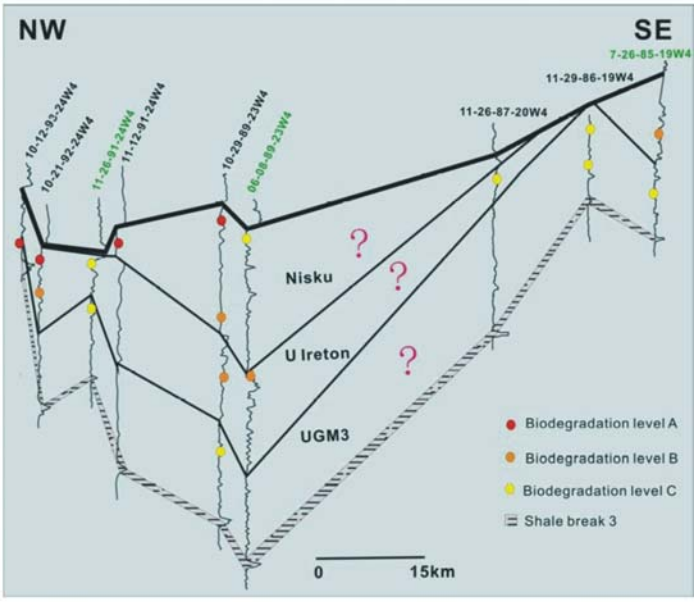

Fig. 14: NW-SE cross-section area to illustrate the biodegradation pattern. Question marks indicate areas that lack sample control. Reproduced from Zhao and Machel (2011).

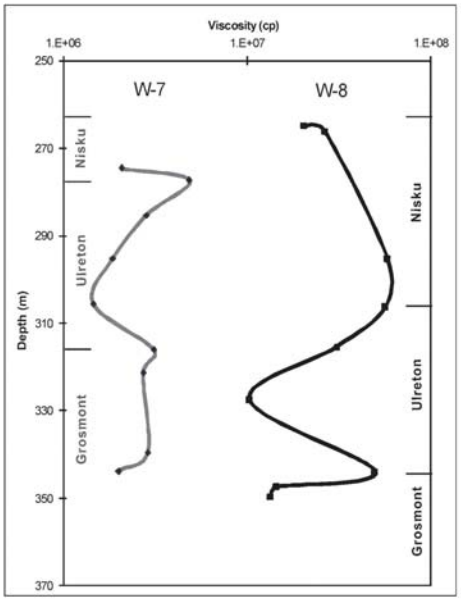

Fig. 15: Zero-shear viscosity in two wells, the left from a fresh core (less than 2 years old), the right from a 'legacy core' (about 30 years old). Note similar depth/stratigraphic variations. From Zhao and Machel (2012).

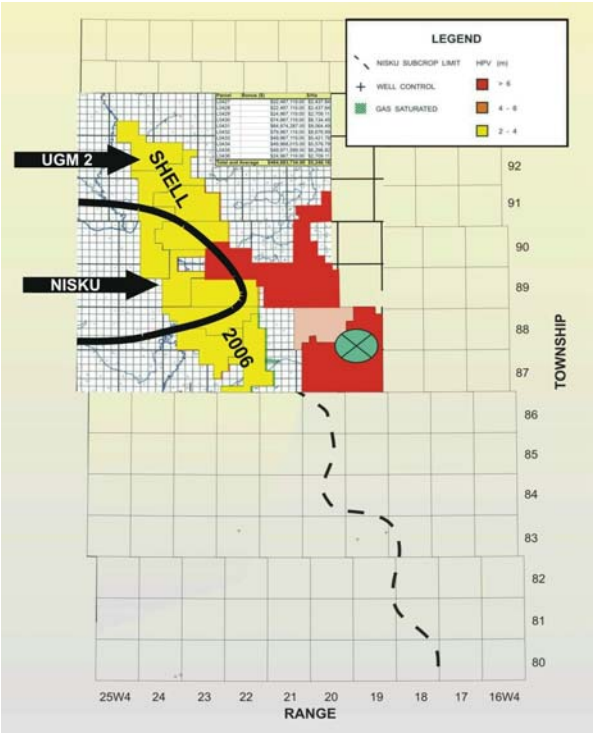

Fig. 16: Map of the northern part of our study area, showing the 'sweet spots' identified by Dembicki (1994) and Dembicki and Machel (1996), as well as the areas leased by Husky (red) and by Shell (yellow) in 2006.